Published in final edited form as:
Cancer Cell. 2015 February 9; 27(2): 257–270. doi:10.1016/j.ccell.2014.12.006.

Glutamate dehydrogenase 1 signals through antioxidant glutathione peroxidase 1 to regulate redox homeostasis and tumor growth

Lingtao Jin[1], **Dan Li**[1], **Gina N. Alesi**[1], **Jun Fan**[1], **Hee-Bum Kang**[1], **Zhou Lu**[2,10], **Titus J. Boggon**[3], **Peng Jin**[4], **Hong Yi**[5], **Elizabeth R. Wright**[6], **Duc Duong**[7], **Nicholas T. Seyfried**[7], **Robert Egnatchik**[8], **Ralph J. DeBerardinis**[8], **Kelly R. Magliocca**[9], **Chuan He**[2], **Martha L. Arellano**[1], **Hanna J. Khoury**[1], **Dong M. Shin**[1], **Fadlo R. Khuri**[1], and **Sumin Kang**[1,*]

[1]Winship Cancer Institute, Department of Hematology and Medical Oncology, Emory University School of Medicine, Atlanta, GA 30322, USA

[2]Department of Chemistry and Institute for Biophysical Dynamics, The University of Chicago, Chicago, IL 60637, USA

[3]Department of Pharmacology, Yale University, New Haven, CT 06520, USA

[4]Department of Human Genetics, Emory University, Atlanta, GA 30322, USA

[5]Robert P. Apkarian Integrated Electron Microscopy Core, Emory University, Atlanta, GA 30322

[6]Department of Pediatrics, Emory University School of Medicine, Atlanta, GA 30322, USA

[7]Department of Biochemistry, Emory University School of Medicine, Atlanta, GA 30322, USA

[8]UT Southwestern Medical Center, Dallas, TX 75390, USA

[9]Department of Pathology & Laboratory Medicine, Emory University School of Medicine, Atlanta, GA 30322, USA

SUMMARY

How mitochondrial glutaminolysis contributes to redox homeostasis in cancer cells remains unclear. Here we report that the mitochondrial enzyme glutamate dehydrogenase 1 (GDH1) is commonly upregulated in human cancers. GDH1 is important for redox homeostasis in cancer cells by controlling the intracellular levels of its product alpha-ketoglutarate (α-KG) and

*Correspondence: smkang@emory.edu; Sumin Kang, Emory University School of Medicine, Atlanta, GA 30322; Tel.: 404-778-1880; Fax: 404-778-5520.
[10]Current address: School of Pharmacy, Fudan University, Shanghai, 201203, China

AUTHOR CONTRIBUTIONS

P.J., M.L.A., H.J.K., D.M.S. and F.R.K. provided critical reagents. Z.L., T.J.B. and C.H. performed structural analyses. H.Y. and E.R.W. performed electron microscopy experiments. D.D. and N.T.S. performed mass spectrometry based assays. R.E. and R.J.D. performed metabolic flux analysis. K.R.M. performed histopathological study. L.J., D.L., G.N.A., J.F., H.-B.K. performed all the other experiments. L.J. and S.K. designed the study and wrote the paper.

subsequent metabolite fumarate. Mechanistically, fumarate binds to and activates a ROS scavenging enzyme glutathione peroxidase 1 (GPx1). Targeting GDH1 by shRNA or a small molecule inhibitor R162 resulted in imbalanced redox homeostasis, leading to attenuated cancer cell proliferation and tumor growth.

INTRODUCTION

Emerging evidence indicates that impaired cellular metabolism is the defining characteristic of nearly all cancers regardless of cellular or tissue origin (Hsu and Sabatini, 2008). One predominant metabolic abnormality is that cancer cells take up glucose at higher rates than normal tissue and favor aerobic glycolysis (Kim and Dang, 2006; Warburg, 1956). In addition to the dependency on glycolysis, cancer cells have another atypical metabolic characteristic, that of increased rates of glutamine metabolism. Although the requirement for mitochondrial ATP production is reduced in glycolytic tumor cells, the demand for TCA cycle-derived biosynthetic precursors and NADPH is unchanged or even increased (Frezza and Gottlieb, 2009). In order to compensate for these changes and to maintain a functional TCA cycle, cancer cells often rely on elevated glutaminolysis.

Glutaminolysis is a mitochondrial pathway that involves the initial deamination of glutamine by glutaminase, yielding glutamate and ammonia. Glutamate is then converted to alpha-ketoglutarate (α-KG), a TCA cycle intermediate, to produce both ATP and anabolic carbons for the synthesis of amino acids, nucleotides, and lipids (DeBerardinis et al., 2007; Lu et al., 2010; Medina, 2001; Moreadith and Lehninger, 1984; Reitzer et al., 1979; Wise and Thompson, 2010). The conversion of glutamate to α-KG is catalyzed by either glutamate dehydrogenase 1 (GDH1, a.k.a. GLUD1, GLUD, GDH) or other transaminases, including glutamate pyruvate transaminase 2 (GPT2, a.k.a. alanine aminotransferase) and glutamate oxaloacetate transaminase 2 (GOT2, a.k.a. aspartate aminotransferase), which convert α-keto acids into their corresponding amino acids in mitochondria (Kovacevic, 1971; Quagliariello et al., 1965). Fluxes of these enzymes are commonly elevated in human cancers (Friday et al., 2011). Glutaminolysis also supports the production of molecules, such as glutathione and NADPH, which protect cells from oxidative stress (DeBerardinis and Cheng, 2010; Reitzer et al., 1979; Wise and Thompson, 2010). Mounting evidence suggests that many types of cancer cells have tumor-specific redox control alterations, with increased levels of reactive oxygen species (ROS) compared to normal cells (Kawanishi et al., 2006; Stuart et al., 2014; Szatrowski and Nathan, 1991; Toyokuni et al., 1995). A moderate increase in ROS can promote cell proliferation and differentiation (Boonstra and Post, 2004), whereas excessive amounts of ROS can cause oxidative damage to proteins, lipid and DNA (Perry et al., 2000). Therefore, maintaining ROS homeostasis is crucial for cell growth and survival. Cells control ROS levels by balancing ROS generation with their elimination by ROS-scavenging systems such as glutathione peroxidase (GPx), gluthathione reductase (GSR), thioredoxin (Trx), superoxide dismutases (SOD), catalase (CAT) and peroxiredoxin (PRX). α-KG, a product of GDH1 and a key intermediate in glutamine metabolism, is known to stabilize redox homeostasis in cells (Niemiec et al., 2011). Although elevated glutaminolysis and altered redox status in cancer cells has been theoretically justified, the

mechanism by which α-KG regulates redox and whether this regulation is crucial for tumorigenesis and tumor growth remain elusive.

RESULTS

GDH1 predominantly regulates α-KG production in cancer cells and is upregulated in human cancers

To better understand the role of glutamine metabolism in human cancers, we tested the effect of blocking the conversion of glutamate to α-KG, a crucial step in glutaminolysis, on cancer cells. Among the three enzymes that may regulate this step, we found that GDH1 is the enzyme predominantly responsible for the conversion of glutamate to α-KG compared to the other two mitochondrial enzymes, GOT2 and GPT2, in lung cancer H1299 cells and breast cancer MDAMB231 cells (Figure 1A). Moreover, shRNA-mediated stable knockdown of GDH1 resulted in a significantly attenuated glutaminolysis rate compared to that in control cells harboring an empty vector (Figure 1B), suggesting a crucial role of GDH1 in glutaminolysis in human cancer cells. Furthermore, we demonstrated that GDH1 expression levels correlate with progressive stages of breast cancer and lung cancer by performing immunohistochemical staining (IHC) using primary tissue microarray samples from breast and lung cancer patients (Figures 1C and 1D, respectively). GDH1 expression levels were significantly increased in the tumor samples from patients with advanced stages of breast or lung cancer compared to adjacent normal tissues from the same patients or normal tissues from individuals with no cancer.

GDH1 is important for cancer cell proliferation and tumor growth

To determine the role of GDH1 in cancer cell proliferation, we generated a group of human cancer cell lines with stable knockdown of GDH1. These included H1299 and MDA-MB231 tumor cells, as well as human leukemia HEL and K562 cells. Non-malignant, proliferating human fetal lung fibroblast MRC-5 and human keratinocyte HaCaT were included as controls. Stable knockdown of GDH1 resulted in decreased cell number in all of the cancer cell lines tested (Figure 2A), but not in control normal proliferating cells (Figure 2B), suggesting a crucial role of GDH1 in cancer cell proliferation. Similar results were obtained from colony formation assay (Figure S1A) and DNA based cell proliferation assay (Figure S1B). Oxidative stress and low glucose culture conditions but not hypoxic conditions further attenuated cell proliferation upon GDH1 knockdown in H1299 lung cancer cells (Figure 2C).

Moreover, we performed a xenograft experiment in which nude mice were subcutaneously injected with H1299 cells harboring an empty vector and H1299 cells with GDH1 knockdown grown on the left and right flanks, respectively. We found that GDH1 knockdown resulted in significantly reduced tumor growth in most of the mice, with 4 out of 9 mice tumor-free, compared to tumors derived from control cells with empty vector (Figures 2D–2E). These results together suggest that GDH1 confers a proliferative advantage to cancer cells and tumor growth.

GDH1 is critical for redox regulation but not bioenergetics or anabolic biosynthesis in cancer cells

To decipher the role of GDH1 in bioenergetics, anabolic biosynthesis, and redox homeostasis of cancer cells, we performed a set of metabolic assays using lung cancer H1299 and breast cancer MDA-MB231 cells with GDH1 knockdown. We found that attenuation of GDH1 in cancer cells did not affect the intracellular ATP levels, compared to control cells harboring an empty vector (Figure S2A). GDH1 knockdown cells showed increased glucose uptake, glycolytic rates and lactate production but unaltered oxygen consumption rate compared to control cells (Figures S2B–S2C). In addition, intracellular ATP level was significantly decreased in GDH1 knockdown cells compared to control cells upon treatment with glycolytic inhibitor, 2-deoxyglucose (2-DG) or glucose deprivation, but not when treated with oligomycin, an inhibitor of oxidative phosphorylation (Figure S2D). These data together suggest that defective glutaminolysis due to GDH1 knockdown allows cells to further rely on glucose catabolism for bioenergetics. Moreover, GDH1 knockdown did not affect oxidative pentose phosphate pathway (PPP) flux (Figure S2E) or the overall lipid or RNA biosynthesis (Figures S2F and S2G). However, knockdown of GDH1 significantly decreased glutamine-dependent RNA biosynthesis, whereas such change of RNA synthesis was not comparable to glucose-derived RNA synthesis (Figure S2G). In contrast, GDH1 knockdown significantly attenuated intracellular ATP levels as well as overall lipid and RNA synthesis levels in cells under stress conditions including low oxygen or low glucose (Figures S2H–S2J), suggesting GDH1 is important in compensating glucose catabolism and oxidation in cells under stress. Nevertheless, since cells with GDH1 knockdown demonstrate reduced cell proliferation and tumor growth under normal conditions, we hypothesized that other metabolic defects such as redox metabolism changes might be responsible for the proliferative disadvantage in cells conferred by GDH1 knockdown.

Indeed, we found that knockdown of GDH1 resulted in increased mitochondrial ROS levels (Figure 3A left) and intracellular H_2O_2 levels (Figure 3A right), while stress conditions induced by H_2O_2 or glucose deprivation resulted in further elevated ROS levels in GDH1 knockdown cells (Figure S2K). In contrast, NADPH levels (Figure 3B left) and the GSH/GSSG ratio (Figure 3B right) were significantly decreased in GDH1 knockdown cells compared to control cells. These data together suggest that GDH1 is important for redox homeostasis in cancer cells, most likely by regulating ROS levels. Consistently, treatment with antioxidant, N-acetylcysteine (NAC) in GDH1 knockdown cells significantly rescued the increased ROS and reduced cell proliferation due to GDH1 deficiency (Figure 3C). Such rescue effects were more apparent under oxidative stress condition induced by H_2O_2 (Figure 3C upper). Next we functionally validated this *in vivo* by performing xenograft experiments. Nude mice were subcutaneously injected with control H1299 cells harboring empty vector or GDH1 knockdown cells. NAC at a concentration of 10 mg/ml was administered via drinking water to half of the mice injected with GDH1 knockdown cells. NAC treatment partially rescued the attenuated tumor growth of H1299 GDH1 knockdown cells in xenograft nude mice (Figure 3D).

To determine whether GDH1 enzyme activity is important for ROS regulation, we next tested whether rescue of reduced intracellular levels of the GDH1 product, α-KG, could reverse the elevated ROS level in GDH1 knockdown cells (Figure 3E). Indeed, cell-permeable methyl-α-KG significantly rescued the attenuated intracellular α-KG (Figure 3E upper), elevated ROS (Figure 3E middle) and decreased cell proliferation (Figure 3E lower) levels in GDH1 knockdown cells. These data suggest that GDH1 requires its enzyme activity to regulate ROS, which contributes to redox homeostasis and cancer cell proliferation.

GDH1 contributes to redox homeostasis in part by regulating glutathione peroxidase (GPx) activity in cancer cells

To investigate how GDH1 regulates ROS levels in cancer cells, we tested whether GDH1 knockdown attenuates any of the known ROS scavenging enzymes, including glutathione peroxidase (GPx), glutathione reductase (GSR), thioredoxin reductase (TRX), superoxide dismutase (SOD), catalase (CAT) and peroxiredoxin (PRX). We found that only GPx enzyme activity is significantly attenuated in GDH1 knockdown MDA-MB231 cells compared to control cells harboring an empty vector (Figure 4A left). Similar results were obtained using lung cancer H1299 cells (Figure 4A right).

To further substantiate that GDH1 controls ROS levels through GPx in cancer cells, we first tested the effect targeting GPx on cell proliferation and ROS level of cancer cells. Although GPx1, GPx3, GPx4, GPx6 and GPx8 exist in human breast cancer cell line MDA-MB231 (Figures S3A and S3B), GPx1 is the predominant isoform that contributes to GPx activity in cancer cells (Figure S3C–S3D). Therefore, we assessed the impact of targeting GPx1. RNAi-mediated downregulation of GPx1 effectively decreased total GPx activity (Figure 4B left). Moreover, knockdown of GPx1 mimicked the effect of GDH1 knockdown, leading to decreased cell proliferation and increased ROS (Figure 4B middle and right). We next tested whether overexpression of active GPx1 can reverse the increased ROS levels and attenuated cell viability in GDH1 knockdown cells. GPx1 is a selenoprotein, which requires a selenocysteine insertion sequence (SECIS) element to translate the UGA codon in the GPx1 gene as selenocysteine (Walczak et al., 1998). We generated a GPx1 construct with a 3’UTR containing the SECIS element to express GPx1 in cells (Figure 4C). We observed that stable overexpression of active GPx1 rescued the attenuated total GPx activity in GDH1 knockdown cells, leading to increased proliferative ability and decreased ROS compared to control GDH1 knockdown cells (Figure 4D). We found that GPx1 colocalizes with GDH1 in the mitochondria (Figures S3E–S3G) and GDH1 regulates GPx1 activity in the mitochondria of cancer cells (Figure S3H).

GDH1 controls fumarate level to potentiate GPx activity

We next explored the molecular mechanism by which GDH1 regulates GPx activity. We found that GDH1 does not form a protein complex with GPx1 (data not shown). We thus hypothesized that GDH1 may indirectly regulate GPx activity and subsequent ROS levels by controlling intracellular levels of α-KG. As shown in Figure 5A, treatment with methyl-α-KG fully rescued the attenuated GPx activity in GDH1 knockdown cells. Next, we incubated purified active GPx1 with physiological concentrations of α-KG (20–80 μM) or other

metabolite intermediates derived from α-KG including fumarate (20–80 μM), succinate (200–500 μM) and malate (200–500 μM) to check whether these metabolites directly affect GPx1 activity *in vitro* (Figure 5B), since each of these metabolites was significantly decreased in cancer cells upon GDH1 knockdown (Figures 1A, 5C, S4A and S4B, respectively). Interestingly, activity of purified human GPx1 either from transient expression in mammalian cells (Figure 5B upper) or human erythrocytes (Figure 5B lower), was significantly increased *in vitro* by fumarate but not the other metabolites. Moreover, treatment with the GDH1 product methyl-α-KG rescued the decreased fumarate in cancer cells, suggesting that GDH1 and its product α-KG control intracellular fumarate levels (Figure 5C). To examine whether fumarate binds to and activates GPx1, we performed a radiometric metabolite-protein interaction analysis using ^{14}C-labeled metabolites incubated with GPx1 enriched from cells. Labeled fumarate but not α-KG, succinate or malate was retained on GPx1, suggesting that fumarate directly binds to GPx1 (Figures 5D and S4C). The K_d value of the GPx1-fumarate interaction was calculated to be 75.52 ± 5.22 μM (Figure S4C). To determine the selectivity of fumarate binding to GPx1, we generated a GPx1 mutant with substitutions at T143 and D144. These residues are predicted to be critical for fumarate binding to GPx1 by a molecular docking study (Figure S4D). Mutational studies demonstrated that GPx1 T143A/D144A (2A) was resistant to fumarate binding and the enzyme activity was no longer enhanced by fumarate (Figures S4E and 5E). This suggests that the GPx1-fumarate interaction is required for fumarate induced GPx1 activation. Furthermore, knockdown of succinate dehydrogenase A (SDHA), which produces fumarate in the TCA cycle abolished the rescue effect of methyl-α-KG in GDH1 knockdown cells (Figure 5F). Consistently, decreased fumarate levels in GDH1 knockdown cells were rescued by cell-permeable dimethyl-fumarate (Figure 5G upper), leading to partially rescued GPx activity and decreased ROS level in these cells (Figure 5G middle and lower, respectively). These data together suggest that GDH1 plays an important role in redox regulation by activating GPx1 through controlling intracellular levels of α-KG and fumarate.

Identification and characterization of R162 as a small molecule inhibitor of GDH1

Our finding that GDH1 is upregulated in human cancers and that attenuation of GDH1 impacts cancer cell proliferation and tumor growth implicates GDH1 as a promising anti-cancer target. Currently the only reported GDH1 inhibitor is epigallocatechin gallate (EGCG), a polyphenol flavonoid isolated from green tea. However, EGCG targets a group of enzymes that use NADPH as a cofactor (Li et al., 2006; Li et al., 2011a; Li et al., 2011b). We thus designed a series of screening assays to identify GDH1-selective inhibitors. We identified a lead small molecule compound, purpurin, as a GDH1 inhibitor from a library of 2,000 FDA-approved small molecule compounds (Figures 6A and S5A–S5C). Purpurin demonstrated dramatic inhibitory effects on the enzyme activity of recombinant, purified active GDH1 proteins in an *in vitro* GDH activity assay with K_i and K_d 1.9 ± 0.26 μM and 11.46 ± 1.17 μM, respectively (Figures 6B–6C left). Although purpurin showed dramatic inhibitory effect on GDH1 enzyme activity *in vitro*, the compound was not cell permeable (Figure S5D). Therefore, we next identified the purpurin analog R162 as a potent GDH1 inhibitor from a group of purpurin derivatives (Figures S5E–S5G and 6B–6C right). R162, which is more cell-permeable than purpurin due to its allyl group, demonstrated more potent

inhibitory effects on mitochondrial GDH activity and elevated ROS levels in cancer cells (Figures 6D and 6E, respectively). Purpurin specifically inhibits activity of GDH but not other NADPH-dependent enzymes such as 6-phosphogluconate dehydrogenase (6PGD) and fumarate hydratase (FH) *in vitro*, whereas EGCG significantly affected activity of 6PGD and FH *in vitro* (Figure S5H). Moreover, comparison of purpurin, R162 and EGCG demonstrated that purpurin and its analog, R162, are more potent and specific for GDH1 inhibition *in vitro* and in cancer cells (Figures S5I–S5K).

To examine the interaction between GDH1 and R162, a thermal melt shift assay was performed. Incubating GDH1 with increasing concentrations of R162 raised the melting temperature (Tm) in a dose dependent manner, suggesting that R162 directly binds to GDH1 (Figure 6F). In addition, in a competitive binding assay where R162 was incubated with purified GDH1 protein in the presence of different concentrations of GDH1 substrate α-KG, the Lineweaver-Burk plot shows that R162 acts as a mixed model inhibitor of GDH1 (Figure 6G).

We also found that inhibition of GDH1 activity by R162 treatment results in decreased intracellular fumarate levels, attenuated GPx activity, increased ROS levels, and reduced cell proliferation in H1299 and MDA-MB231 cells, which could be significantly rescued by methyl-α-KG treatment (Figure 6H) as well as by antioxidant NAC (Figure 6I). These data are essentially consistent with the phenotypes observed in GDH1 knockdown cells, suggesting that R162 targets GDH1 to disrupt redox balance through GPx1 and inhibit cancer cell proliferation.

R162 dramatically attenuated cell viability in a group of human lung cancer, breast cancer and leukemia cell lines, but not in human proliferating cells including human keratinocyte (HaCaT), human fetal lung fibroblast (MRC-5), and human foreskin fibroblast cells (HFF), which serve as control proliferative human cells (Figure 7A). Furthermore, inhibiting GDH1 by R162 also resulted in decreased cell viability of primary leukemia cells from myeloid leukemia patients, but did not affect cell viability of mononucleocytes in peripheral blood samples from healthy human donors (Figure 7B). These data suggest the anti-proliferative potential of R162 in human cancer cells with minimal toxicity.

Next we tested the *in vivo* efficacy of R162 in the treatment of xenograft tumor mouse models. For initial *in vivo* toxicity studies, 30 mg/kg/day of R162 was administered to mice for 30 days by intraperitoneal injection. The chronic R162 treatment did not result in a significant histopathological change between the vehicle-treated and R162-treated groups (Figure 7C), nor altered complete blood counts, or hematopoietic properties (Figure 7D), suggesting minimal toxicity of R162 *in vivo*. Therefore, we performed an *in vivo* R162 treatment using H1299-xenograft nude mice. A day after xenograft injection, mice were divided into two groups (n=8/group) and treated with either R162 (20 mg/kg/day) or control DMSO for 35 days. R162 treatment resulted in significantly decreased tumor growth and masses in mice compared with control mice (Figure 7E). Moreover, R162 effectively inhibited GDH1 activity in resected tumors from xenograft nude mice (Figure 7F). These results together suggest that R162 is a GDH1 inhibitor with promising anti-proliferative potential in cancer cells with minimal toxicity *in vitro* and *in vivo*.

DISCUSSION

Our findings suggest a mechanism by which the mitochondrial GDH1 contributes to redox homeostasis. GDH1 controls the intracellular levels of its product α-KG and the subsequent metabolic intermediate fumarate, which binds and activates the ROS scavenging enzyme GPx1, providing metabolic advantages to cancer cell proliferation and tumor growth (Figure 8). Although three enzymes including GDH1, GOT2 and GPT2 are reported to convert glutamate to α-KG (Kovacevic, 1971; Quagliariello et al., 1965), our results demonstrate that GDH1 plays a predominant role in maintaining the physiological levels of α-KG in cancer cells. GDH1 may also play a critical role in α-KG-dependent biological functions, including not only the TCA cycle but also epigenetic regulations involving diverse α-KG-dependent enzymes such as histone and DNA dioxygenases that regulate genome-wide histone and DNA methylation (Loenarz and Schofield, 2008; Simmons et al., 2008).

Emerging evidence has demonstrated the importance of glutamine as an alternative carbon source for both bioenergetics and anabolic biosynthesis in addition to glucose. Consistently, our results showed that suppression of GDH1 resulted in decreased glutaminolysis, which renders cancer cells more dependent on glycolysis and more sensitive to stress conditions such as glucose deprivation, but not low oxygen. Moreover, although GDH1 deficiency resulted in decreased biosynthesis of lipids and RNA derived from glutamine, such changes in biosynthesis are dispensable to cancer cells when glucose dependent biosynthesis is predominant under normal, stress-free conditions. These metabolic changes are either advantageous (increased glycolysis) or dispensable (biosynthesis) to cancer cells. However, the GDH1 knockdown cells still showed decreased cell proliferation and tumor growth, suggesting that other severe metabolic defects due to GDH1 deficiency eventually overshadow these changes. Our findings showing that GDH1 regulates redox homeostasis through GPx1 shed insights into the current understanding of the biological functions of GDH1, and reveal a distinct crosstalk between glutaminolysis and redox maintenance.

Moreover, our finding that fumarate binds to and activates GPx1 provides another example to support an emerging mechanism in which metabolic intermediates may function as signaling molecules to allow crosstalk between metabolic and cell signaling pathways (Hitosugi et al., 2012; Sanders et al., 2007). A recent report demonstrates that FH loss increases fumarate levels and results in mitochondrial ROS activation in FH-deficient renal carcinoma cells (Sullivan et al., 2013). This implies that the role of fumarate may depend on cancer type and discrete TCA cycle conditions, such as intracellular fumarate levels. Our findings, along with others, showcase the complicated signaling properties in cancer cells that coordinate metabolic and cell signaling networks to provide ultimately optimized proliferative advantages to cancer cells. Future studies are warranted to decipher the structural basis by which fumarate regulates GPx activity.

Targeting GDH1 with shRNA or a small molecule inhibitor R162 led to reduced cancer cell proliferation and tumor growth. Treatment with the cell permeable GDH1 product, methyl-α-KG, significantly rescued these phenotypes. However, rescue of α-KG level by methyl-α-KG significantly but not completely reversed decreased cell proliferation in GDH1 knockdown cells, suggesting that the effects of GDH1 on cell proliferation are dependent

not only on enzyme activity but also on protein level. In addition, antioxidant NAC treatment reversed ROS levels to that of control cells, but could not completely rescue the reduced cell proliferation or tumor growth in GDH1 knockdown cells. This suggests that GDH1 regulates not only redox status but also other cellular properties that contribute to the regulation of cancer cell proliferation and tumor growth. Future studies are warranted to further investigate the GDH1 enzyme-independent signaling mechanism, which confers cancer cell proliferation and tumor growth.

Recent studies have suggested that targeting the Rho GTPase signaling-dependent glutaminase (GLS), the first enzyme in the glutaminolysis process that converts glutamine to glutamate, effectively suppresses the growth of cancer cells (Wang et al., 2010). Inhibition of glutaminase with another GLS inhibitor bis-2-[5-phenylacetamido-1,2,4-thiadiazol-2-yl] ethyl sulfide (BPTES), also attenuated growth of glioma cells with mutant IDH1 (Robinson et al., 2007; Seltzer et al., 2010). Our studies show that attenuation of GDH1, commonly upregulated in human cancers, specifically reduced breast cancer, lung cancer, and leukemia cell proliferation but not that of non-malignant human proliferating cells. Here we report that targeting GDH1 regulates both glutaminolysis and redox balance in cancer cells, suggesting GDH1 as an attractive anti-cancer target. Although the anti-oxidant polyphenol flavonoid, EGCG, is reported to inhibit GDH1 activity, it is a general inhibitor of NADPH-dependent enzymes. Our small molecule R162 has promising efficacy in inhibiting cancer cell proliferation as well as primary leukemia cells from patients with minimal cytotoxic effects to human cells. R162 also has promising efficacy *in vivo* with minimal toxicity. Our present studies provide a proof-of-principle that GDH1 could be a promising alternative therapeutic target for the clinical treatment of human cancers that rely heavily on glutamine metabolism. Further *in vivo* toxicity of these small molecule GDH1 inhibitors in metabolically active organs such as brain, heart and liver needs to be tested and detailed pharmacokinetics studies will be needed. These well-characterized GDH1 inhibitors will also be powerful chemical tools to further understand how GDH1 regulates cancer metabolism and tumor growth.

EXPERIMENTAL PROCEDURES

Reagents

Lentiviral short hairpin RNA (shRNA) targeting GDH1, GOT2, and GPT2 and GDH1 image clone were purchased from Open Biosystems. SDHA siRNA was from Qiagen. Human GPx1 with 3'UTR region was myc or flag tagged by PCR and subcloned into pLHCX-derived Gateway destination vector. The GPx1 variant was generated by Site-directed mutagenesis kit (Aligent Technologies). Mitochondria were isolated from cells using a mitochondria isolation kit (Pierce). Purified GDH from human erythrocytes was obtained from Sigma-Aldrich. ^{14}C-fumaric acid (60 mCi/mMol) was obtained from Moravek Biochemicals. ^{14}C-ketoglutaric acid (58.7 mCi/mMol) was from Perkin Elmer. All chemicals were purchased from Sigma-Aldrich unless specifically indicated.

Antibodies

Antibodies against GDH1, GOT2, GPT2, GPx1, PRX3 and Ki-67 were purchased from Abcam. Anti-catalase, anti-TRX1, anti-SDHA and anti-myc antibodies were obtained from Cell Signaling Technology. Antibodies against GSR and SOD2 were obtained from Santa Cruz Biotechnology and BD Biosciences, respectively. Anti-FLAG and Anti-β-actin antibodies were obtained from Sigma-Aldrich.

Cell Culture

H1299, A549, HEL, KG1a, Molm14, K562 cells were cultured in RPMI 1640 medium with 10% fetal bovine serum (FBS). 293T, MDA-MB231, SKBR3, HaCaT, HFF and MRC-5 cells were cultured in Dulbecco Modified Eagle Medium (DMEM) with 10% FBS. Lentivirus production, cell infection for RNAi and protein overexpression in human cells and stable cell selection were described previously (Jin et al., 2013).

Enzyme Activity Assays

GDH enzyme activity assay was performed as previously described (Zaganas et al., 2002). Briefly, 20 μg of total cell lysates or 100 ng of purified GDH1 was added to the reaction mixture containing 50 mM triethanolamine pH 8.0, 100 mM ammonium acetate, 100 μM NADPH and 2.6 mM EDTA. The reaction was initiated by adding α-KG and the activity was assessed by monitoring the oxidation of NADPH as a decrease in absorbance at 340 nm. Glutathione peroxidase (GPx), superoxide dismutase (SOD), thioredoxin reductase (TRX), glutathione reductase (GSR), and catalase (CAT) enzyme activities were determined by using commercially available kits from Biovision according to the manufacturer's instructions. Peroxiredoxin (PRX) enzyme activity was assayed by coupling its activity to oxidation of NADPH via thioredoxin reductases (Nelson and Parsonage, 2011).

Glutaminolysis Rate Measurement

Glutamine oxidation assay measuring $^{14}CO_2$ from ^{14}C glutamine was used to determine glutaminolysis rate. Briefly, cells were seeded on 6-cm dishes that were placed in a sealed 10-cm dish. Cells were incubated with 4 μCi/ml of [U-^{14}C] glutamine for 4 hr and the reaction was stopped by the addition of 200 μl of 70% perchloric acid, which also released CO_2. 0.5 ml of 3 M NaOH was injected to a cup placed next to the 6-cm dish to absorb all the released CO_2 from the cells and after 12 hr incubation, 20 μl of NaOH was subjected to liquid scintillation counting.

Intracellular ATP, Lactate production, and Oxygen Consumption Assays

Intracellular ATP concentration was measured by using an ATP bioluminescent somatic cell assay kit (Sigma-Aldrich). 5×10^5 cells were suspended in ultrapure water. The reaction was initiated by adding ATP enzyme mix to the cell suspension and the luminescence was recorded by spectrofluorometer (Molecular Probe). Cellular lactate production was measured with a fluorescence-based lactate assay kit (MBL). Plain phenol red-free RPMI medium was added to subconfluent cells for 1 hr and the media was assessed for lactate level. The values were normalized with cell number. Oxygen consumption rates were

measured using a clark-type microcathode oxygen electrode attached to a 782 oxygen meter (Strathkelvin Instruments).

Intracellular ROS, NADPH level, and GSH/GSSG ratio Measurements

Total intracellular Cellular ROS was determined by staining the cells with carboxy-H_2DCFDA (Invitrogen) and mitochondrial ROS level was determined by using a specific mitochondrial H_2O_2 probe, MitoPY1 (Sigma) as previously described (Dickinson and Chang, 2008; Dickinson et al., 2013). 2×10^5 cells were incubated with 10 μM carboxy-H_2DCFDA or 10 μM of MitoPY1 for 30 min at 37°C. Cells were washed and analyzed by flow cytometry (BD FACSCanto). Intracellular NADPH level and GSH/GSSG ratio were determined using fluorimetric SensoLyte NADP/NADPH Assay (AnaSpec) and GSH/GSSG-Glo™ (Promega), respectively.

Intracellular Metabolite Measurements

The intracellular levels of α-KG, fumarate, succinate, and malate were determined by using commercial kits (Biovision). Briefly, 2×10^6 cells were homogenized in PBS. The supernatant was collected and proteins were removed by using 10 KD Amicon Ultra Centrifugal Filters (Millipore). The flow-through containing the metabolites was used for the measurement of α-KG, fumarate, succinate, and malate, following the manufacturer's instructions.

Radiometric ^{14}C-fumarate/^{14}C-α-KG – GPx1 Binding Assay

Bead-bound flag-GPx1 purified from transfected 293T cell lysates was washed with TBS buffer (50 mM Tris, 150 mM NaCl, pH 7.5), followed by incubation with 0.12 μCi ^{14}C-fumarate or ^{14}C-α-KG for 30 min in TBS buffer. The beads were then washed with TBS buffer. The bead-bound GPx1 protein was eluted with 10 μg flag peptides and radioactivity was detected by liquid scintillation counting.

Cell Proliferation Assay

5×10^4 adherent cells or 1×10^5 leukemia cells were seeded in 6-well plate and cell numbers were determined by trypan blue exclusion using TC10 automated cell counter (Bio-Rad). For α-KG, NAC, and R162 treatment experiments, cells were treated with different concentrations of α-KG, NAC and R162, followed by cell counting as mentioned above.

Xenograft Studies

Animal experiments were performed according to protocols approved by the Institutional Animal Care and Use Committee of Emory University. Nude mice (athymic nu/nu, female, 4–6 weeks old, Harlan) were subcutaneously injected with 1×10^7 H1299 cells harboring empty vector on the left flank, and cells with stable knockdown of GDH1 on the right flank, respectively. For the NAC rescue experiment, mice of the NAC rescue group were treated with NAC drinking water at 10 mg/ml from 3 days after H1299-GDH1 shRNA cells injection for 42 days. To evaluate the efficacy of R162, the drug was administered from a day after H1299 cells injection by daily intraperitoneal injection of 30 mg/kg for 35 days. 50% of DMSO in PBS was as a diluent control. Tumor growth was recorded by

measurement of two perpendicular diameters of the tumors and tumor size was calculated using the formula $4\pi/3 \times (\text{width}/2)^2 \times (\text{length}/2)$. The tumors were harvested and weighed at the experimental endpoint. Tumor proliferation was determined by Ki-67 IHC staining.

Drug Screening using *in vitro* GDH Assay

To screen potential GDH1 inhibitors, *in vitro* GDH1 activity assay was performed as described above in presence of compounds (10 μM) using GDH1-overexpressing 293T cell lysates or purified GDH (Sigma). Detailed screening strategy and results are shown in Supplemental Data Figure S7.

GDH1 Enzyme Kinetics

2 μM purified GDH1 was incubated with different concentrations of purpurin or R162 in 50 mM Tris-Cl buffer (pH 7.5) and intrinsic tryptophan fluorescence (Ex:280 nm/Em:350 nm) was measured for Tryptophan fluorescence binding assay. Nonlinear regression analysis was performed using Prism 6 (GraphPad) to calculate dissociation constant (K_d). Inhibition constants (Ki) of purpurin and R162 were determined by GDH activity assay with different concentrations of substrate, α-KG, and computed by using Prism 6 (GraphPad).

Thermal Shift Assay

Thermal shift assay was performed using the Protein Thermal Shift Dye Kit (Life Technologies). 10 μM of purified GDH was incubated with different concentrations of R162 and protein-drug mixture was added to the reaction mixture. The fluorescence was recorded using Real-Time PCR Systems (Applied Biosystems) and data were analyzed using Protein Thermal Shift Software v1.0 (Life Technologies).

Tissue Microarray Analysis

Paraffin embedded breast cancer and lung cancer tissue microarrays were obtained from US Biomax. IHC analysis of GDH1 expression was performed according to the protocol described previously (Li et al., 2013). Approval of use of human specimens was given by the Institutional Review Board of Emory University. All clinical samples were collected with informed consent under Health Insurance Portability and Accountability Act (HIPAA) approved protocols.

Statistical Analysis

Statistical analysis and graphical presentation was performed using Prism 6 (GraphPad). Data shown are from one representative experiment of multiple independent experiments and are given as mean ± SD, except for tumor growth curves which represent mean ± SEM. Statistical analysis of significance was based on the one-way analysis of variance (One-Way ANOVA) for Figures 1C–1D and two-tailed Student's *t* test for all the other figures.

Supplementary Material

Refer to Web version on PubMed Central for supplementary material.

ACKNOWLEDGEMENTS

We acknowledge Dr. Anthea Hammond for editorial assistance. We thank the Integrated Cellular Imaging Core of Emory University. This work was supported in part by NIH grants R01 CA175316 (S.K.), F31 CA183365 (G.A.), and S10 RR025679 01 (P.S.), ACS grant RSG-11-081-01 (S.K.), Georgia Cancer Coalition (H.J.K.) and the Hematology Tissue Bank of the Emory University School of Medicine. G.A. is an NIH pre-doctoral fellow. H.J.K., F.R.K., and S.K. are Georgia Cancer Coalition Scholars. S. K is a Robbins Scholar and an American Cancer Society Basic Research Scholar.

REFERENCES

Boonstra J, Post JA. Molecular events associated with reactive oxygen species and cell cycle progression in mammalian cells. Gene. 2004; 337:1–13. [PubMed: 15276197]

DeBerardinis RJ, Cheng T. Q's next: the diverse functions of glutamine in metabolism, cell biology and cancer. Oncogene. 2010; 29:313–324. [PubMed: 19881548]

DeBerardinis RJ, Mancuso A, Daikhin E, Nissim I, Yudkoff M, Wehrli S, Thompson CB. Beyond aerobic glycolysis: transformed cells can engage in glutamine metabolism that exceeds the requirement for protein and nucleotide synthesis. Proc Natl Acad Sci U S A. 2007; 104:19345–19350. [PubMed: 18032601]

Dickinson BC, Chang CJ. A targetable fluorescent probe for imaging hydrogen peroxide in the mitochondria of living cells. Journal of the American Chemical Society. 2008; 130:9638–9639. [PubMed: 18605728]

Dickinson BC, Lin VS, Chang CJ. Preparation and use of MitoPY1 for imaging hydrogen peroxide in mitochondria of live cells. Nature protocols. 2013; 8:1249–1259.

Frezza C, Gottlieb E. Mitochondria in cancer: not just innocent bystanders. Semin Cancer Biol. 2009; 19:4–11. [PubMed: 19101633]

Friday E, Oliver R 3rd, Welbourne T, Turturro F. Glutaminolysis and glycolysis regulation by troglitazone in breast cancer cells: Relationship to mitochondrial membrane potential. J Cell Physiol. 2011; 226:511–519. [PubMed: 20683912]

Hitosugi T, Zhou L, Elf S, Fan J, Kang HB, Seo JH, Shan C, Dai Q, Zhang L, Xie J, et al. Phosphoglycerate mutase 1 coordinates glycolysis and biosynthesis to promote tumor growth. Cancer cell. 2012; 22:585–600. [PubMed: 23153533]

Hsu PP, Sabatini DM. Cancer cell metabolism: Warburg and beyond. Cell. 2008; 134:703–707. [PubMed: 18775299]

Jin L, Li D, Lee JS, Elf S, Alesi GN, Fan J, Kang HB, Wang D, Fu H, Taunton J, et al. p90 RSK2 mediates antianoikis signals by both transcription-dependent and - independent mechanisms. Molecular and cellular biology. 2013; 33:2574–2585. [PubMed: 23608533]

Kawanishi S, Hiraku Y, Pinlaor S, Ma N. Oxidative and nitrative DNA damage in animals and patients with inflammatory diseases in relation to inflammation-related carcinogenesis. Biological chemistry. 2006; 387:365–372. [PubMed: 16606333]

Kim JW, Dang CV. Cancer's molecular sweet tooth and the Warburg effect. Cancer Res. 2006; 66:8927–8930. [PubMed: 16982728]

Kovacevic Z. The pathway of glutamine and glutamate oxidation in isolated mitochondria from mammalian cells. The Biochemical journal. 1971; 125:757–763. [PubMed: 4401609]

Li C, Allen A, Kwagh J, Doliba NM, Qin W, Najafi H, Collins HW, Matschinsky FM, Stanley CA, Smith TJ. Green tea polyphenols modulate insulin secretion by inhibiting glutamate dehydrogenase. J Biol Chem. 2006; 281:10214–10221. [PubMed: 16476731]

Li C, Li M, Chen P, Narayan S, Matschinsky FM, Bennett MJ, Stanley CA, Smith TJ. Green tea polyphenols control dysregulated glutamate dehydrogenase in transgenic mice by hijacking the ADP activation site. J Biol Chem. 2011a; 286:34164–34174. [PubMed: 21813650]

Li D, Jin L, Alesi GN, Kim YM, Fan J, Seo JH, Wang D, Tucker M, Gu TL, Lee BH, et al. The prometastatic ribosomal S6 kinase 2-cAMP response element-binding protein (RSK2-CREB) signaling pathway up-regulates the actin-binding protein fascin-1 to promote tumor metastasis. J Biol Chem. 2013; 288:32528–32538. [PubMed: 24085294]

Li M, Li C, Allen A, Stanley CA, Smith TJ. The structure and allosteric regulation of mammalian glutamate dehydrogenase. Arch Biochem Biophys. 2011b

Loenarz C, Schofield CJ. Expanding chemical biology of 2-oxoglutarate oxygenases. Nature chemical biology. 2008; 4:152–156.

Lu W, Pelicano H, Huang P. Cancer metabolism: is glutamine sweeter than glucose? Cancer cell. 2010; 18:199–200. [PubMed: 20832746]

Medina MA. Glutamine and cancer. J Nutr. 2001; 131:2539S–2542S. discussion 2550S-2531S. [PubMed: 11533309]

Moreadith RW, Lehninger AL. The pathways of glutamate and glutamine oxidation by tumor cell mitochondria. Role of mitochondrial NAD(P)+-dependent malic enzyme. J Biol Chem. 1984; 259:6215–6221. [PubMed: 6144677]

Nelson KJ, Parsonage D. Measurement of peroxiredoxin activity. Current protocols in toxicology / editorial board, Mahin D Maines. 2011; 7(Unit7):10.

Niemiec T, Sikorska J, Harrison A, Szmidt M, Sawosz E, Wirth-Dzieciolowska E, Wilczak J, Pierzynowski S. Alpha-ketoglutarate stabilizes redox homeostasis and improves arterial elasticity in aged mice. Journal of physiology and pharmacology : an official journal of the Polish Physiological Society. 2011; 62:37–43. [PubMed: 21451208]

Perry G, Raina AK, Nunomura A, Wataya T, Sayre LM, Smith MA. How important is oxidative damage? Lessons from Alzheimer's disease. Free radical biology & medicine. 2000; 28:831–834. [PubMed: 10754280]

Quagliariello E, Papa S, Saccone C, Palmieri F, Francavilla A. The Oxidation of Glutamate by Rat-Liver Mitochondria. The Biochemical journal. 1965; 95:742–748. [PubMed: 14342510]

Reitzer LJ, Wice BM, Kennell D. Evidence that glutamine, not sugar, is the major energy source for cultured HeLa cells. J Biol Chem. 1979; 254:2669–2676. [PubMed: 429309]

Robinson MM, McBryant SJ, Tsukamoto T, Rojas C, Ferraris DV, Hamilton SK, Hansen JC, Curthoys NP. Novel mechanism of inhibition of rat kidney-type glutaminase by bis-2-(5-phenylacetamido-1,2,4-thiadiazol-2-yl)ethyl sulfide (BPTES). The Biochemical journal. 2007; 406:407–414. [PubMed: 17581113]

Sanders MJ, Grondin PO, Hegarty BD, Snowden MA, Carling D. Investigating the mechanism for AMP activation of the AMP-activated protein kinase cascade. The Biochemical journal. 2007; 403:139–148. [PubMed: 17147517]

Seltzer MJ, Bennett BD, Joshi AD, Gao P, Thomas AG, Ferraris DV, Tsukamoto T, Rojas CJ, Slusher BS, Rabinowitz JD, et al. Inhibition of glutaminase preferentially slows growth of glioma cells with mutant IDH1. Cancer Res. 2010; 70:8981–8987. [PubMed: 21045145]

Simmons JM, Muller TA, Hausinger RP. Fe(II)/alpha-ketoglutarate hydroxylases involved in nucleobase, nucleoside, nucleotide, and chromatin metabolism. Dalton transactions. 2008:5132–5142. [PubMed: 18813363]

Stuart SD, Schauble A, Gupta S, Kennedy AD, Keppler BR, Bingham PM, Zachar Z. A strategically designed small molecule attacks alpha-ketoglutarate dehydrogenase in tumor cells through a redox process. Cancer & metabolism. 2014; 2:4. [PubMed: 24612826]

Sullivan LB, Martinez-Garcia E, Nguyen H, Mullen AR, Dufour E, Sudarshan S, Licht JD, Deberardinis RJ, Chandel NS. The proto-oncometabolite fumarate binds glutathione to amplify ROS-dependent signaling. Molecular cell. 2013; 51:236–248. [PubMed: 23747014]

Szatrowski TP, Nathan CF. Production of large amounts of hydrogen peroxide by human tumor cells. Cancer Res. 1991; 51:794–798. [PubMed: 1846317]

Toyokuni S, Okamoto K, Yodoi J, Hiai H. Persistent oxidative stress in cancer. FEBS letters. 1995; 358:1–3. [PubMed: 7821417]

Walczak R, Carbon P, Krol A. An essential non-Watson-Crick base pair motif in 3'UTR to mediate selenoprotein translation. Rna. 1998; 4:74–84. [PubMed: 9436910]

Wang JB, Erickson JW, Fuji R, Ramachandran S, Gao P, Dinavahi R, Wilson KF, Ambrosio AL, Dias SM, Dang CV, Cerione RA. Targeting mitochondrial glutaminase activity inhibits oncogenic transformation. Cancer cell. 2010; 18:207–219. [PubMed: 20832749]

Warburg O. On the origin of cancer cells. Science. 1956; 123:309–314. [PubMed: 13298683]

Wise DR, Thompson CB. Glutamine addiction: a new therapeutic target in cancer. Trends Biochem Sci. 2010; 35:427–433. [PubMed: 20570523]

Zaganas I, Spanaki C, Karpusas M, Plaitakis A. Substitution of Ser for Arg-443 in the regulatory domain of human housekeeping (GLUD1) glutamate dehydrogenase virtually abolishes basal activity and markedly alters the activation of the enzyme by ADP and L-leucine. J Biol Chem. 2002; 277:46552–46558. [PubMed: 12324473]

Significance

Our findings provide insight into understanding the role of glutaminolysis in redox homeostasis. We demonstrated that GDH1 predominantly controls the intracellular levels of α-KG in cancer cells and plays a crucial role in redox homeostasis. Moreover, our findings also suggest a unique signaling function of fumarate that regulates GPx1, allowing additional crosstalk between glutaminolysis, TCA cycle and redox status. Finally, our GDH1 inhibitor R162 demonstrated promising efficacy and minimal toxicity in the treatment of diverse human cancer cells *in vitro* and *in vivo*, as well as in primary leukemia cells from human patients. Thus, our findings provide proof-of-principle suggesting GDH1 as a promising therapeutic target in the treatment of human cancers associated with elevated glutamine metabolism.

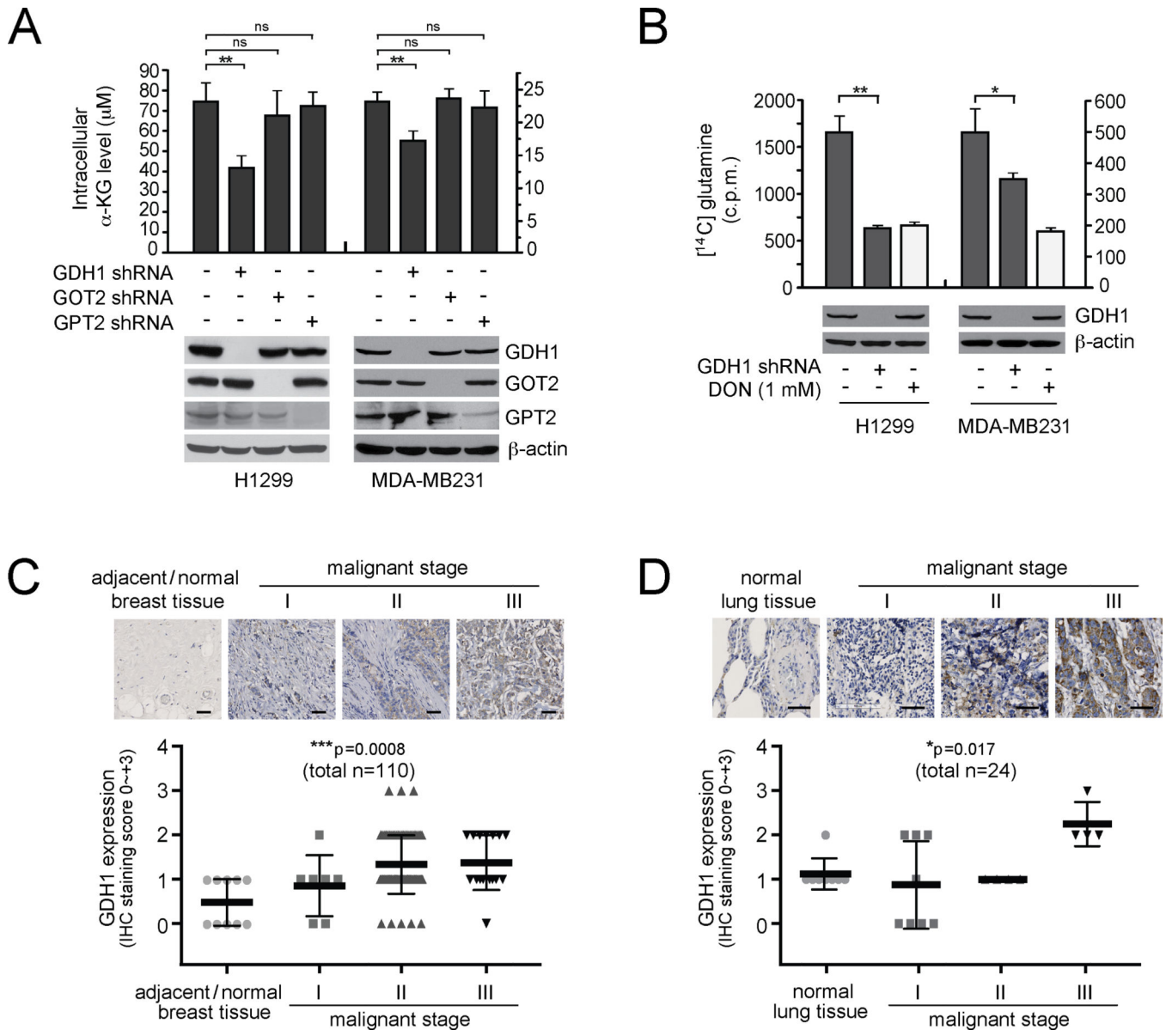

Figure 1. GDH1 predominantly regulates α-KG production in cancer cells and is upregulated in human lung and breast cancers

(A) Intracellular α-KG levels were determined in human lung cancer H1299 and breast cancer MDA-MB231 cells with stable knockdown of GDH1, GOT2, or GPT2. Expression of GDH1, GOT2 and GPT2 in H1299 and MDA-MB231 cells are shown by Western blot analyses. β-actin was used as a loading control. **(B)** Glutaminolytic rates in H1299 and MDA-MB231 cells were determined with stable knockdown of GDH1 or control cells harboring an empty vector. DON (6-diazo-5-oxo-I-norleucine), glutamine antagonist, was used as a positive control. GDH1 expression is shown by Western blotting. Data are mean ± SD from three replicates of each sample and p values were determined by a two-tailed paired Student's *t* test for panels 1A and 1B (ns: not significant; *: $0.01 < p < 0.05$; **: $0.001 < p < 0.01$). **(C–D)** Immunohistochemistry analyses of GDH1 expression in groups of primary human tissue specimens. Tissue microarrays of breast ductal carcinoma (C) and

lung cancer (D) were obtained from US biomax. Scale bars = 50 μm. Data are mean ± SD. p values were obtained by ANOVA test. (*: $0.01 < p < 0.05$; ***: $p < 0.001$).

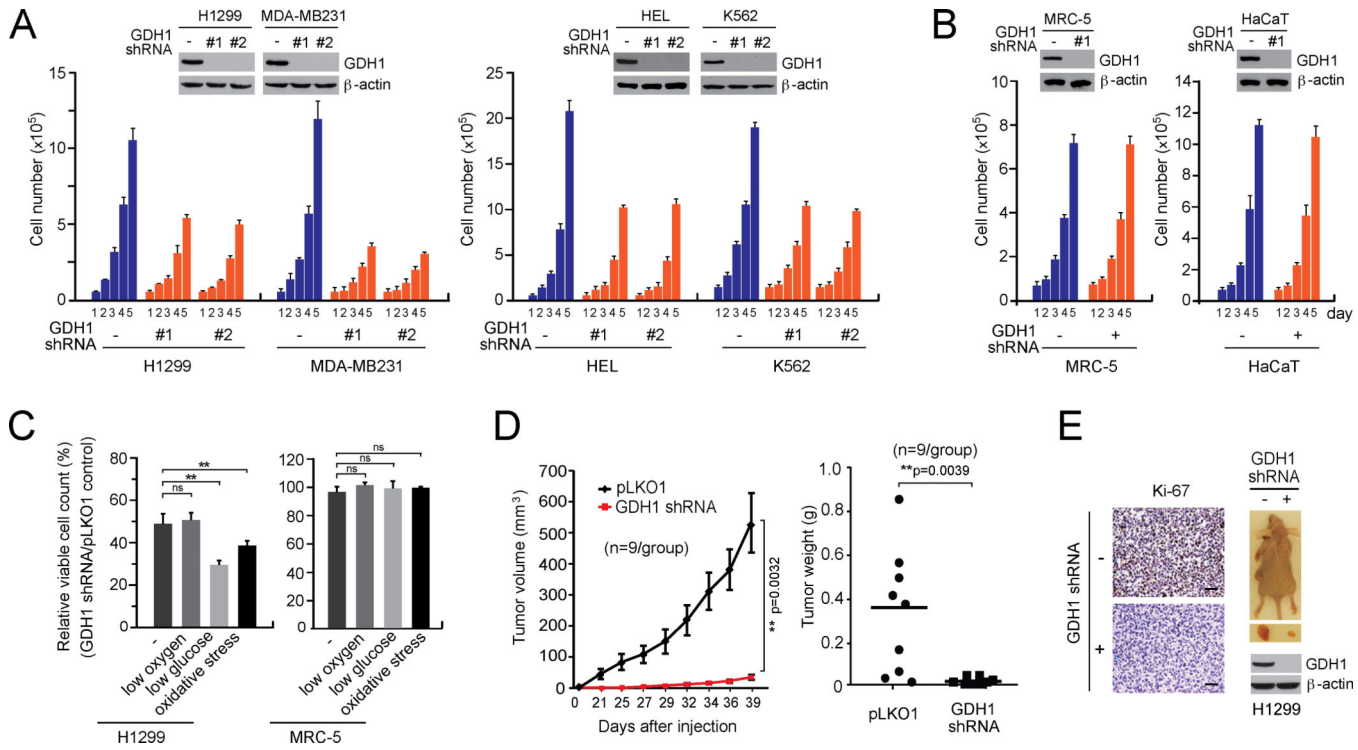

Figure 2. GDH1 is important for cancer cell proliferation and tumor growth

(A–B) Cell proliferation rates were determined by cell counting in H1299 and MDA-MB231 tumor cells (A; *left*), HEL and K562 leukemia cells (A; *right*) and MRC-5 and HaCaT (B) with stable knockdown of GDH1, compared to control cells expressing an empty vector. Expression of GDH1 in cells transduced with GDH1 shRNA clones are shown by Western blot analyses. **(C)** Effect of GDH1 knockdown on cell proliferation rates were measured under stress conditions including low oxygen (1% O_2), low glucose (0.5 mM glucose) and oxidative stress (15 μM H_2O_2). **(D)** Effect of GDH1 knockdown on tumor growth potential of H1299 cell xenograft mice. *Left:* Tumor size was monitored every 2–3 days for 6 weeks. The error bars represent SEM. *Right:* Tumor weights were examined at the experimental endpoint. **(E)** *Left:* Representative pictures of IHC staining to detect Ki-67 expression in tumors harvested from vector control group or GDH1 knockdown group. Scale bars = 50 μm. *Right:* Representative dissected tumors and GDH1 expression in tumor lysates are shown. Data are mean ± SD from three replicates of each sample except panels D and E. p values were determined by a twotailed Student's *t* test for panel C and a two-tailed paired Student's *t* test for panel D (ns: not significant; **: 0.001 < p < 0.01). See also Figure S1.

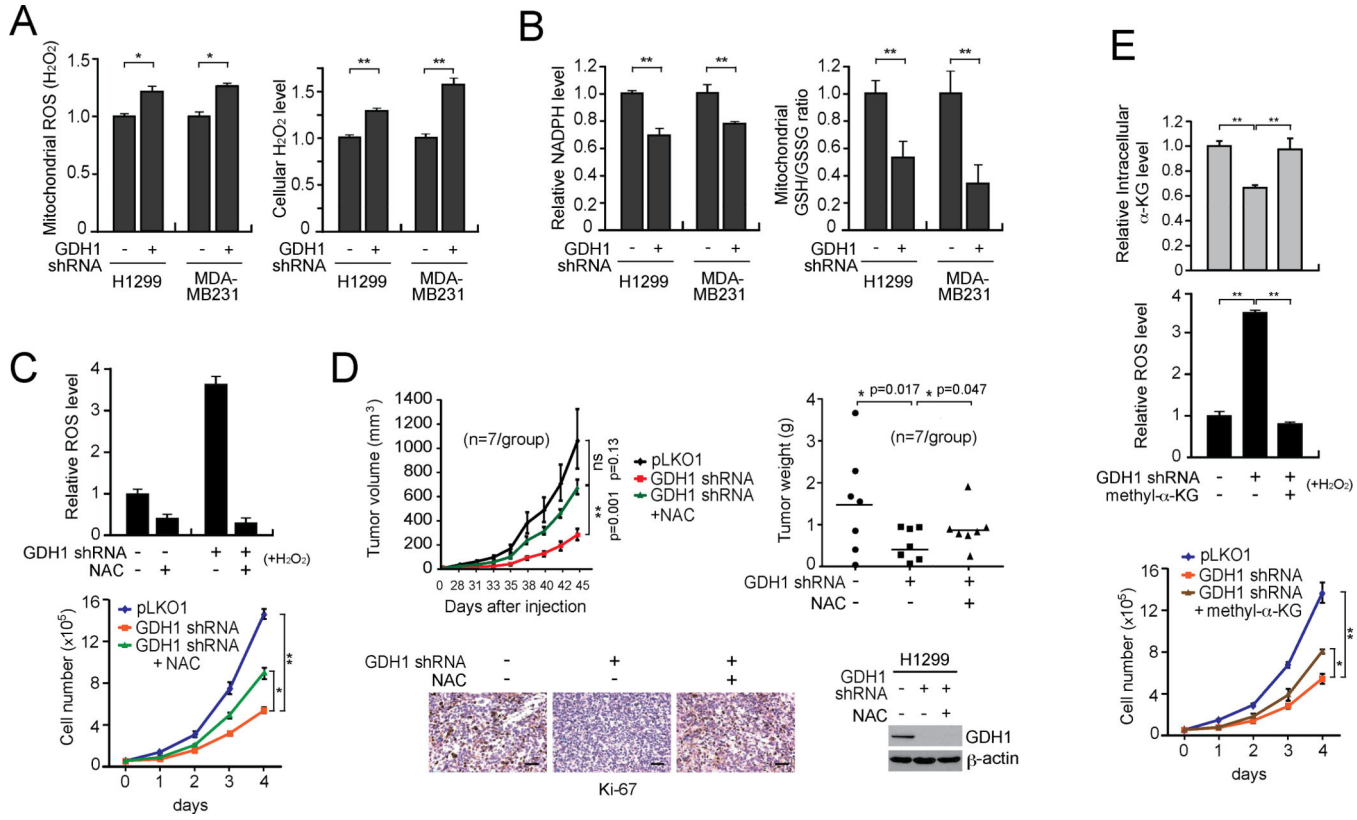

Figure 3. GDH1 contributes to redox homeostasis in cancer cells

(A–B) Mitochondrial ROS and cellular H_2O_2 levels (A), NADPH levels and mitochondrial GSH/GSSG ratio (B) were determined in H1299 and MDA-MB231 cells with GDH1 knockdown or control cells with an empty vector. **(C)** H1299 cells with GDH1 knockdown were treated with anti-oxidant agent NAC (1 mM). ROS (*upper*) and cell proliferation (*lower*) were measured. **(D)** NAC (10 mg/ml drinking water) was administrated in H1299 xenograft mice with GDH1 knockdown. *Upper left:* Tumor growth was monitored. The error bars represent SEM. *Upper right:* Tumor weights were examined at the experimental endpoint. *Lower left:* Representative pictures of Ki-67 IHC staining of tumor samples. Scale bars = 50 μm. *Lower right:* GDH1 expression in tumor lysates is shown. **(E)** H1299 cells were treated in the presence and absence of 0.5 mM methyl-α-KG. Intracellular α-KG level (*upper*), ROS production (*middle*) and proliferation rates (*lower*) were determined as described above. Data are mean ± SD from three replicates except panel D. p values were determined by a two-tailed Student's *t* test (ns: not significant; *: 0.01 < p < 0.05; **: 0.001 < p < 0.01). See also Figure S2.

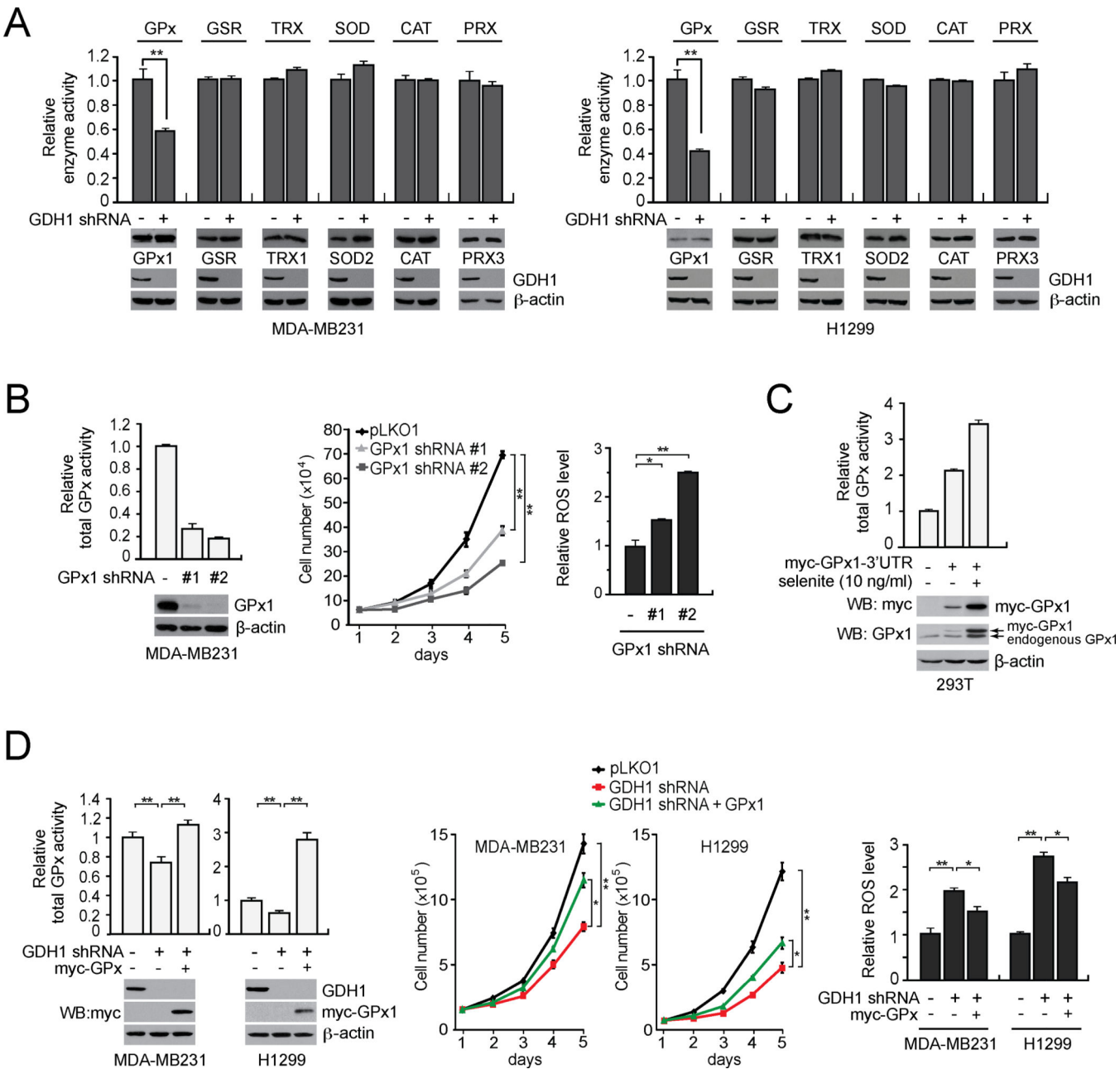

Figure 4. GDH1 contributes to redox homeostasis in part by regulating glutathione peroxidase (GPx) activity in cancer cells

(A) Effect of GDH1 knockdown on the enzyme activity of GPx and other ROS scavenging enzymes including GSR, TRX, SOD, CAT and PRX in MDA-MB231 (*left*) and H1299 (*right*) cells. Western blots displaying the expression of GPx1, GSR, TRX1, SOD2, CAT, PRX3 and GDH1 in cells with GDH1 stable knockdown or an empty vector. β-actin was used as a loading control. **(B)** Effect of GPx1 knockdown on total GPx activity (*left*), cell proliferation (*middle*) and ROS (*right)* in MDA-MB231 cancer cells. Knockdown efficiency of GPx1 was determined by Western blotting. Cell proliferation rates and ROS levels were assessed by cell counting and carboxy-H_2DCFDA detection, respectively. **(C)** Induction of

GPx1 expression in 293T cells transduced with a GPx1 expression construct harboring a 3'UTR with a SECIS element that responds to selenite. Expression of myc tagged GPx1 was determined by immunoblotting using anti-myc and anti-GPx1 antibodies. **(D)** Effect of myc-GPx1 stable expression on the total cellular GPx activity (*left*), cell proliferation (*middle*) and ROS (*right*) in MDA-MB231 and H1299 cells with stable knockdown of GDH1. 10 ng/ml selenite was added in the culture media for all the assays. GDH1 knockdown and myc-GPx1 expression is shown by Western blot analyses. Data are mean ± SD from three replicates. p values were determined by a two-tailed Student's *t* test (*$0.01 < p < 0.05$; **$0.001 < p < 0.01$). See also Figure S3.

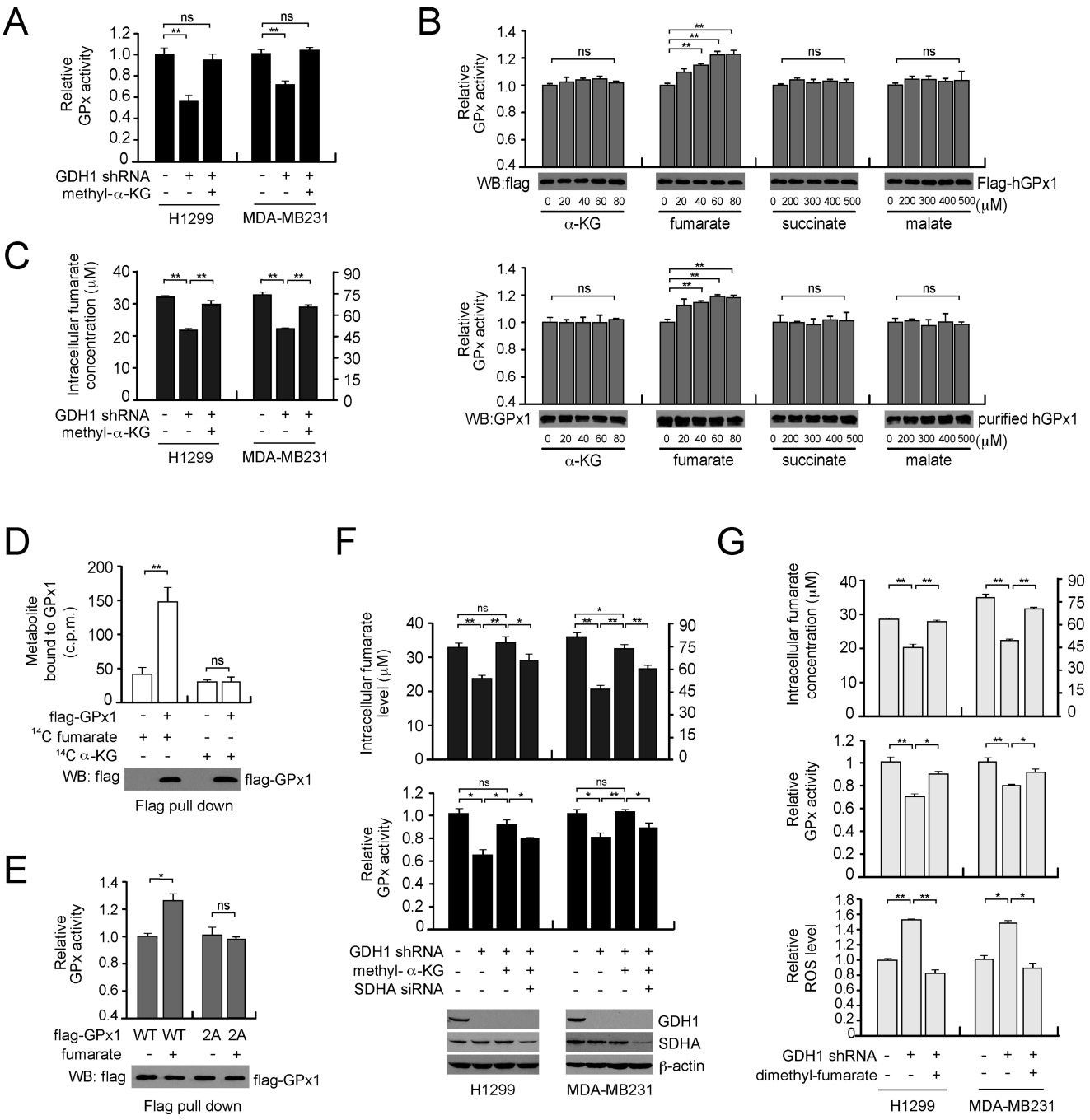

Figure 5. GDH1 promotes GPx activity by controlling intracellular fumarate level

(A) GPx activity in cancer cells with stable knockdown of GDH1 was determined in the presence or absence of cell-permeable methyl-α-KG. **(B)** The activity of purified flag-GPx1 from 293T cells or endogenous GPx1 from human erythrocytes was examined in the presence of increasing concentrations of α-KG, fumarate, succinate or malate. Western blot analyses show GPx1 input for each sample. **(C)** Effect of methyl-α-KG treatment on intracellular fumarate level in GDH1 knockdown cells. **(D)** Flag-GPx1 was pulled down from transfected 293T cell lysates and incubated with ^{14}C-fumarate or ^{14}C-α-KG. The

unbound metabolites were washed away and retained fumarate or α-KG was measured using a scintillation counter. Western blot analysis shows GPx1 input for each sample. **(E)** The activity of purified flag-GPx1 wild-type (WT) or fumarate binding deficient mutant flag-GPx1 T143A/D144A (2A) from 293T cells was examined in the presence of fumarate (80 μM). Western blot analysis shows GPx1 input for each sample. **(F)** Intracellular fumarate levels *(upper)* and relative enzyme activity of endogenous GPx (*lower*) in GDH1 knockdown cells were determined in the presence or absence of methyl-α-KG and SDHA siRNA. Knockdown of GDH1 and SDHA is shown by Western blot analyses. **(G)** Intracellular fumarate levels (*upper*), GPx activity (*middle*) and ROS levels (*lower*) in cancer cells with stable knockdown of GDH1 were determined in the presence or absence of cell-permeable dimethyl-fumarate. Data are mean ± SD from three replicates. p values were determined by two-tailed Student's *t* test (ns: not significant; *$0.01 < p < 0.05$; **$0.001 < p < 0.01$). See also Figure S4.

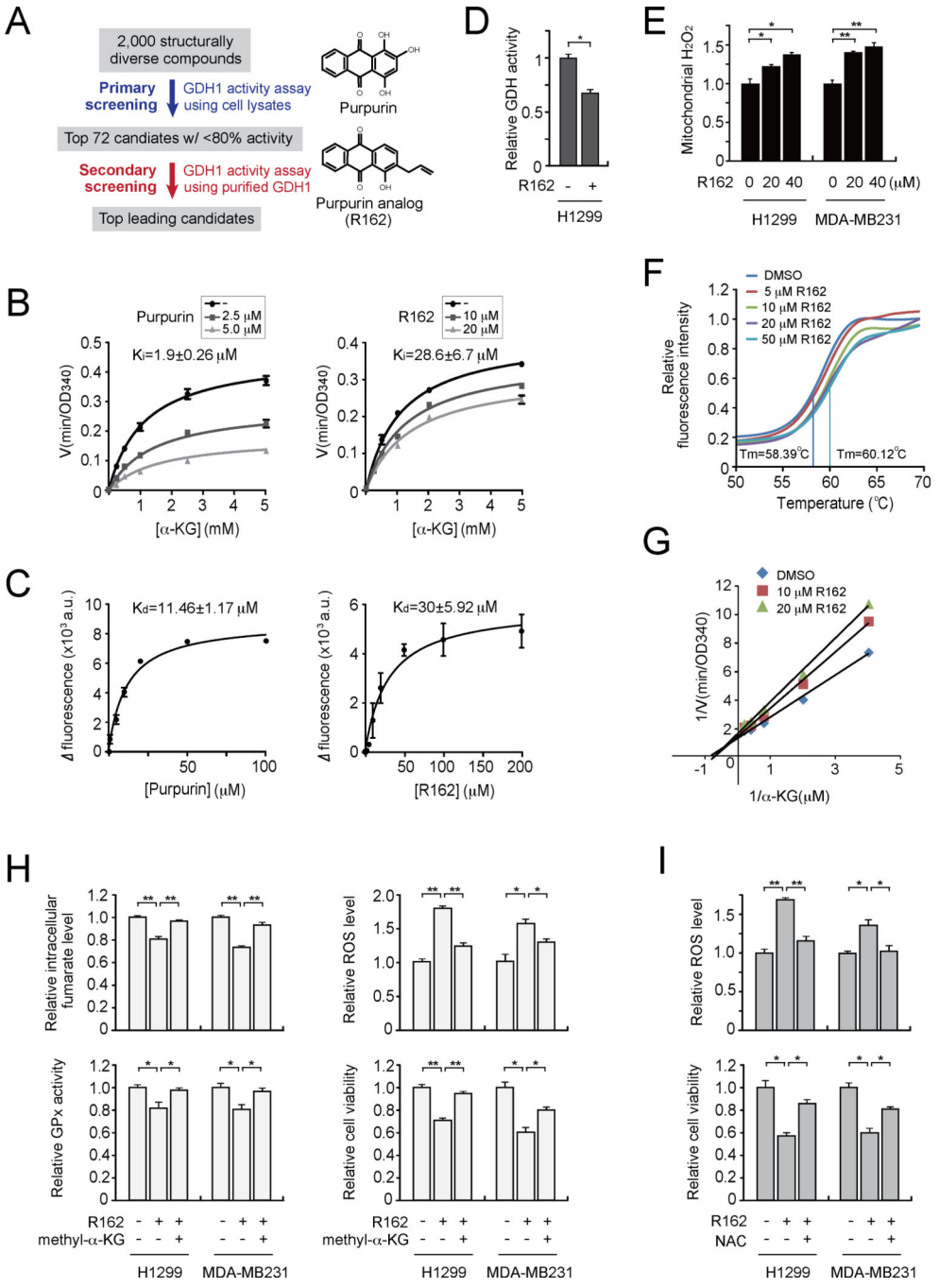

Figure 6. Identification and characterization of R162 as a small molecule inhibitor of GDH1

(A) *Left:* Schematic illustration of screening strategies used to identify lead compounds as GDH1 inhibitors. *Right:* Structures of purpurin and its derivative R162. **(B)** Activity of purified GDH1 in the presence of different concentrations of α-KG and purpurin (*left*) or R162 (*right*). **(C)** K_d values were determined by tryptophan fluorescence binding assay. Purified GDH1 was incubated with increasing concentrations of purpurin (*left*) or R162 (*right*). **(D)** GDH activity was determined in cancer cells treated with R162 (20 μM). **(E)** Mitochondrial ROS levels were determined in H1299 and MDA-MB231 cells in the

presence of R162. **(F)** Thermal shift melting curve of purified GDH1 incubated with increasing concentrations of R162. Melting temperature (Tm) of DMSO control and 50 μM R162 are indicated. **(G)** Lineweaver-Burk plot of GDH activity in the presence of increasing concentrations of R162 and α-KG. **(H)** Effects of methyl-α-KG treatment (1 mM) on intracellular fumarate level (*upper left*), GPx activity (*lower left*), ROS level (*upper right*) and cell proliferation (*lower right*) in R162-treated H1299 and MDA-MB231 cells were examined. **(I)** Effect of NAC treatment (3 mM) on ROS level (*upper*) and cell proliferation (*lower*) in R162-treated cells. Data are mean ± SD from three replicates. p values were determined by a two-tailed Student's *t* test (*$0.01 < p < 0.05$; **$0.001 < p < 0.01$). See also Figure S5.

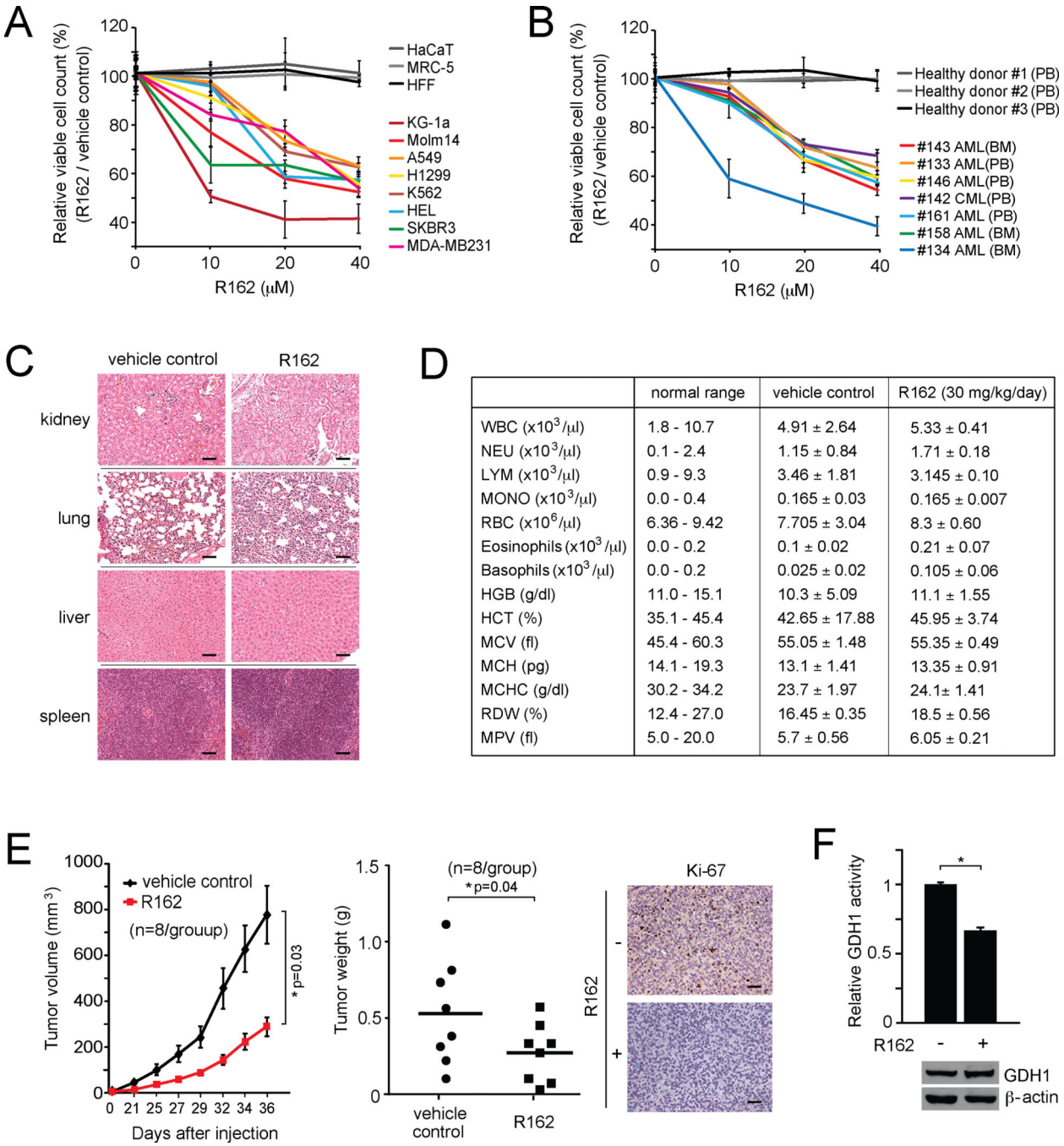

	normal range	vehicle control	R162 (30 mg/kg/day)
WBC (x10^3/μl)	1.8 - 10.7	4.91 ± 2.64	5.33 ± 0.41
NEU (x10^3/μl)	0.1 - 2.4	1.15 ± 0.84	1.71 ± 0.18
LYM (x10^3/μl)	0.9 - 9.3	3.46 ± 1.81	3.145 ± 0.10
MONO (x10^3/μl)	0.0 - 0.4	0.165 ± 0.03	0.165 ± 0.007
RBC (x10^6/μl)	6.36 - 9.42	7.705 ± 3.04	8.3 ± 0.60
Eosinophils (x10^3 /μl)	0.0 - 0.2	0.1 ± 0.02	0.21 ± 0.07
Basophils (x10^3 /μl)	0.0 - 0.2	0.025 ± 0.02	0.105 ± 0.06
HGB (g/dl)	11.0 - 15.1	10.3 ± 5.09	11.1 ± 1.55
HCT (%)	35.1 - 45.4	42.65 ± 17.88	45.95 ± 3.74
MCV (fl)	45.4 - 60.3	55.05 ± 1.48	55.35 ± 0.49
MCH (pg)	14.1 - 19.3	13.1 ± 1.41	13.35 ± 0.91
MCHC (g/dl)	30.2 - 34.2	23.7 ± 1.97	24.1± 1.41
RDW (%)	12.4 - 27.0	16.45 ± 0.35	18.5 ± 0.56
MPV (fl)	5.0 - 20.0	5.7 ± 0.56	6.05 ± 0.21

Figure 7. R162 inhibits cell proliferation and tumor growth potential of human cancer cells

(A) Cell viability of diverse human tumor and leukemia cells in the presence of R162. Control cells include HaCaT, MRC-5 and HFF. **(B)** Effect of R162 treatment on cell viability of human primary leukemia cells from patients with myeloid leukemia. Peripheral blood cells from healthy donors were included as controls. BM: bone marrow; PB: peripheral blood; AML: Acute myeloid leukemia; CML: Chronic myeloid leukemia. **(C)** Histological analysis of hematoxylin-eosin stained tissue sections of representative mice in R162 or vehicle control treated group. Scale bars = 50 μm. Mice were treated with R162 (30

mg/kg/day) for 30 days. **(D)** Hematology blood test of R162 or vehicle control treated mice. **(E)** Effect of R162 administration on tumor growth in H1299 xenograft mice model. *Left:* Tumor growth was monitored. The error bars represent SEM. *Middle:* Tumor weight was examined at the experimental endpoint. *Right:* Representative pictures of Ki-67 IHC staining of tumor samples from control or R162 treatment group. Scale bars = 50 μm. **(F)** GDH1 protein and activity levels were determined in dissected tumor samples. Representative pictures of dissected tumors are shown. GDH1 expression in tumor lysates is shown by Western blotting. Data are mean values ± SD from three replicates except panels C and E. p values were determined by a two-tailed Student's *t* test (*$0.01 < p < 0.05$).

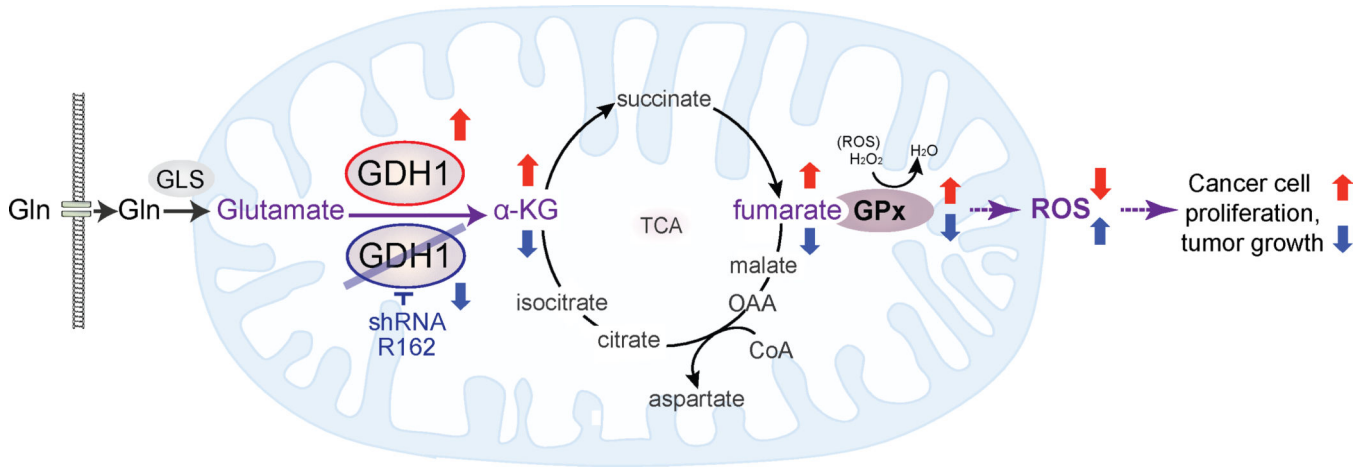

Figure 8. Proposed model for the role of GDH1 in cancer metabolism

Upregulated GDH1 in cancer cells is critical to maintain the physiological levels of α-KG and consequently fumarate. Fumarate may in turn bind to and activate the ROS scavenging enzyme GPx to regulate redox homeostasis, which provides a proliferative advantage to cancer cells and tumor growth. In contrast, suppression of GDH1 decreased α-KG and fumarate levels, leading to reduced GPx activity and subsequently elevated ROS that attenuates cancer cell proliferation and tumor growth.